Dissolution: The Achilles' Heel of the Triton Shell in an Acidifying Ocean

著者（英）	Paul Harvey Benjamin, Sylvain AGOSTINI, Shigeki WADA, Kazuo INABA, Jason M. Hall-Spencer
journal or publication title	Frontiers in Marine Science
volume	5
page range	371
year	2018-10
権利	(C)2018 Harvey, Agostini, Wada, Inaba and Hall-Spencer. This is an open-access article distributed under the terms of the Creative Commons Attribution License (CC BY). The use, distribution or reproduction in other forums is permitted, provided the original author(s) and the copyright owner(s) are credited and that the original publication in this journal is cited, in accordance with accepted academic practice. No use, distribution or reproduction is permitted which does not comply with these terms. Frontiers
URL	http://hdl.handle.net/2241/00157211

doi: 10.3389/fmars.2018.00371

frontiers in Marine Science

ORIGINAL RESEARCH
published: 12 October 2018
doi: 10.3389/fmars.2018.00371

Dissolution: The Achilles' Heel of the Triton Shell in an Acidifying Ocean

Ben P. Harvey[1], Sylvain Agostini[1], Shigeki Wada[1], Kazuo Inaba[1] and Jason M. Hall-Spencer[1,2]**

[1] Shimoda Marine Research Center, University of Tsukuba, Shimoda, Japan, [2] Marine Biology and Ecology Research Centre, University of Plymouth, Plymouth, United Kingdom

Ocean acidification is expected to negatively impact many calcifying marine organisms by impairing their ability to build their protective shells and skeletons, and by causing dissolution and erosion. Here we investigated the large predatory "triton shell" gastropod *Charonia lampas* in acidified conditions near CO_2 seeps off Shikine-jima (Japan) and compared them with individuals from an adjacent bay with seawater pH at present-day levels (outside the influence of the CO_2 seep). By using computed tomography we show that acidification negatively impacts their thickness, density, and shell structure, causing visible deterioration to the shell surface. Periods of aragonite undersaturation caused the loss of the apex region and exposing body tissues. While gross calcification rates were likely reduced near CO_2 seeps, the corrosive effects of acidification were far more pronounced around the oldest parts of the shell. As a result, the capacity of *C. lampas* to maintain their shells under ocean acidification may be strongly driven by abiotic dissolution and erosion, and not under biological control of the calcification process. Understanding the response of marine calcifying organisms and their ability to build and maintain their protective shells and skeletons will be important for our understanding of future marine ecosystems.

Keywords: dissolution, ocean acidification, CO_2 seeps, *Charonia lampas*, triton shell, calcifying organisms, CT-scanning

OPEN ACCESS

Edited by:
Christopher Edward Cornwall, Victoria University of Wellington, New Zealand

Reviewed by:
Nina Bednarsek, Southern California Coastal Water Research Project, United States
Jeff C. Clements, University of New Brunswick, Canada

****Correspondence:***
Ben P. Harvey
harvey.benjaminpaul@gmail.com
Jason M. Hall-Spencer
jason.hall-spencer@plymouth.ac.uk

Specialty section:
This article was submitted to Global Change and the Future Ocean, a section of the journal Frontiers in Marine Science

Received: *28 May 2018*
Accepted: *25 September 2018*
Published: *12 October 2018*

Citation:
Harvey BP, Agostini S, Wada S, Inaba K and Hall-Spencer JM (2018) Dissolution: The Achilles' Heel of the Triton Shell in an Acidifying Ocean. Front. Mar. Sci. 5:371. doi: 10.3389/fmars.2018.00371

INTRODUCTION

Surface seawater is being altered due to increasing atmospheric carbon dioxide (CO_2) concentrations, causing reductions in pH, carbonate ions [CO_3^{2-}], and saturation states (Ω) of calcium carbonate minerals (Raven et al., 2005; IPCC, 2013). This fundamental change to sea water chemistry is termed ocean acidification (Caldeira and Wickett, 2003) and can make seawater corrosive to carbonates. Over this century, many calcifying marine organisms may be negatively impacted by ocean acidification as it is expected to impair their ability to build and maintain protective shells and skeletons (Harvey et al., 2013; Kroeker et al., 2013; Gattuso et al., 2015). As calcifying organisms are a fundamental component of coastal marine communities, the effects of ocean acidification are expected to lead to profound ecological shifts (Hall-Spencer et al., 2008; Harvey et al., 2014; Nagelkerken and Connell, 2015; Sunday et al., 2017).

Calcification refers to the process by which calcifying marine organisms use dissolved ions to construct calcium carbonate ($CaCO_3$) shells and skeletons. It is now thought that the effects of ocean acidification on calcification are not an issue of [CO_3^{2-}] substrate limitation (Bach, 2015; Cyronak et al., 2016; Waldbusser et al., 2016); instead representing a physiological constraint

(Cyronak et al., 2016; Waldbusser et al., 2016). Many organisms use bicarbonate ions [HCO_3^-] or CO_2 in the production of $CaCO_3$ (Roleda et al., 2012), so increased levels of dissolved inorganic carbon may allow some taxa to maintain or even increase their calcification rates (Wood et al., 2008; Ries et al., 2009; Rodolfo-Metalpa et al., 2011). However, ocean acidification increases the concentration of protons in seawater, making it more energetically expensive for some organisms to maintain internal pH homeostasis (Stumpp et al., 2012). The degree of control that species have over their internal carbonate chemistry will determine their ability to calcify in the lower carbonate saturation conditions caused by ocean acidification (Cohen and Holcomb, 2009; Ries et al., 2009).

Calcification may be counteracted by dissolution of exposed shell or skeleton in areas where waters become corrosive to carbonates for example due to shoaling of the lysocline in the deep-sea, or in polar waters, in upwelling areas, and in regions influenced by low salinity (Feely et al., 2008; Nienhuis et al., 2010; Rodolfo-Metalpa et al., 2011). Dissolution rates of unprotected carbonates exposed to seawater will increase over the coming century as saturation state (Ω) declines (Morse and Arvidson, 2002; IPCC, 2013), with relatively soluble minerals (aragonite and high-Mg calcite) affected more readily than the low-Mg calcite form of calcium carbonate (Morse et al., 2007). Corrosion of exposed shells or skeletons can also be expected in living organisms if their food supply is limited (Thomsen et al., 2013) or their feeding behaviour is negatively affected (Harvey and Moore, 2016; Clements and Darrow, 2018) since less energy can be allocated to upregulate calcification. The metabolic cost of maintenance of shells and skeletons is expected to increase (Barry et al., 2011; Fitzer et al., 2014) and require reallocation of energy away from other key physiological processes such as reproduction, growth, or immune function (Wood et al., 2008; Garilli et al., 2015; Harvey and Moore, 2016; Harvey et al., 2016). The ability of calcifying organisms to develop normally will depend on their capacity to maintain calcification.

The molluscan shell has gained prominence historically in the analysis of calcification processes because it is geometrically simple, yet diverse in form and mineralogy (Kohn et al., 1979). In most gastropods, the epidermis of the mantle deposits new shell material accumulatively onto the existing aperture, resulting in shell growth that coils spirally. Widely used measures of shell growth are shell length and surface area. However, since many calcified organisms can develop malformations and reductions in shell thickness, density, and strength in response to ocean acidification (Nienhuis et al., 2010; Rodolfo-Metalpa et al., 2011; Queirós et al., 2015; Chatzinikolaou et al., 2016), it is not always suitable to rely on such simple measurements alone. Moreover, different gastropod shell regions (apex, body whorl, and shell lip) may not respond in the same manner. Given that shell deterioration is gradual, impacts might shift from net dissolution at the oldest part of the shell to net calcification at the outer shell lip (Chatzinikolaou et al., 2016), explaining why shell apices are often eroded or truncated in ocean acidification studies (e.g., Garilli et al., 2015; Queirós et al., 2015; Chatzinikolaou et al., 2016).

Japanese volcanic CO_2 seeps are starting to be used to show how organisms in Asia will respond to ocean acidification *in situ* and for extended periods (Inoue et al., 2013; Agostini et al., 2018). Here, we compared *Charonia lampas* (Linnaeus, 1758) living in acidified shallow-water conditions near CO_2 seeps off Japan with individuals at sites with seawater pH at present-day levels (outside the influence of the CO_2 seep) to assess their ability to cope with acidification. This species is a gastropod from the Ranellidae (tritons and trumpet shells) family; it was first described in the Mediterranean and is widely distributed throughout the Atlantic, Indian, and Pacific Oceans, including Asia. Adult tritons are large predatory gastropods that inhabit coral reefs and rocky substrata, typically feeding upon starfish, holothurians, and sea urchins (Kang and Kim, 2004). We examined how ocean acidification influences their shell structure and integrity using computed tomography (CT) scanning with particular focus on shell thickness, density, morphology, and dissolution across different shell regions.

MATERIALS AND METHODS

Sampling

Live *C. lampas* were collected by scuba diving off *RV Tsukuba II* in June *2016* on rocky substrata at around 8 m depth in a bay on the south of the small island Shikine-jima, Japan (34°19′17″ N, 139°12′17″ E). The largest ten individuals seen on a 1 h dive were collected from a seep site at mean pH_T 7.789 ± 0.096 [SD; n = 4160, measurements every 15 min] where maximum, mean, and minimum aragonite saturation ($\Omega_{aragonite}$) were 2.31, 1.76, and 0.73, respectively (**Figure 1** and **Table 1**). Here the gastropods were easy to find as they had gleaming white shells. The same protocol was used to collect ten individuals from a reference site, although it took 3 h diving to find them as they were much better camouflaged by a dark periostracum and an extensive cover of epiphytes (mainly crustose coralline algae). The reference site seawater at 6 m depth had mean pH_T 8.137 ± 0.056 [SD; n = 1963, measurements every 30 min] where maximum, mean, and minimum aragonite saturation were 5.29, 3.30, and 2.36, respectively (**Figure 1** and **Table 1**). After collection, the gastropods were immediately frozen at −20°C, the soft body parts were then removed, the inside of the shell rinsed with a solution of 10% sodium hypochlorite, and water, and then left to dry. Carbonate chemistry was calculated using pH_T and temperature data continuously measured using a Durafet sensor (SeaFET, Sea-Bird Scientific, Halifax, Canada), and salinity was measured using a hobo conductivity logger (U24-002-C, Bourne, Onset, United States) at each site from 26th May 2016 to July 5th 2016 (see Agostini et al., 2018 for full details, including the temporal variability in pH and temperature). Total alkalinity (A_T) samples were collected as discrete samples (seep site, n = 41; reference site, n = 52) and immediately filtered at 0.45 μm using disposable cellulose acetate philtres (Dismic, Advantech, Japan). Total alkalinity was then measured by titration (785 DMP Titrino, Metrohm) with HCl at 0.1 mol L^{-1}. Carbonate chemistry parameters were calculated using CO2SYS (Pierrot et al., 2006). Measured pH, A_T, temperature, and salinity were

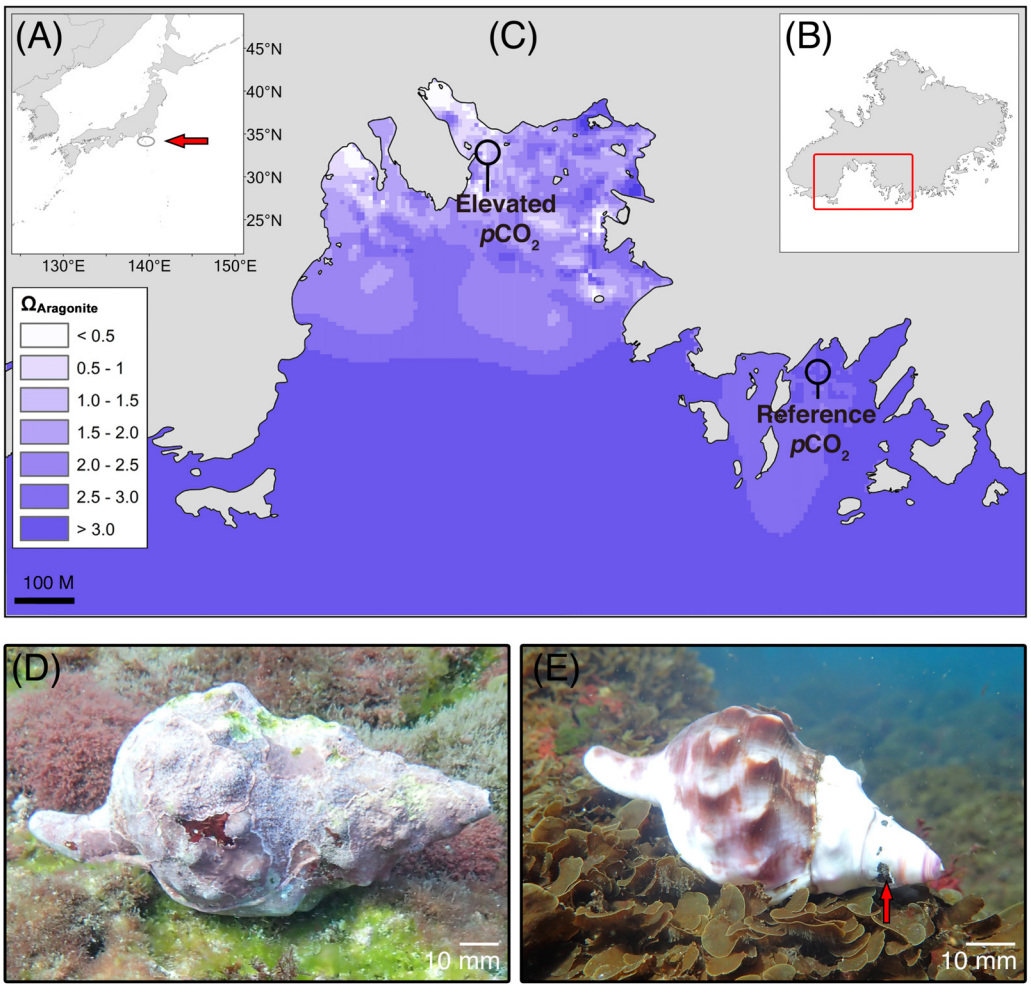

FIGURE 1 | Study area (Mikama Bay, Shikine-jima, Japan) for the collection of *Charonia lampas*. **(A)** Location within Japan (arrow), **(B)** location of Mikama Bay on Shikine-jima, and **(C)** aragonite saturation state (Ω_{Arag}) of the study site (modified from data in Agostini et al., 2018 using ArcGIS "spline with barriers" interpolation tool), with the collection areas for the "elevated pCO_2" individuals (near CO_2 seeps) and "reference pCO_2" individuals from an adjacent bay highlighted. Representative *Charonia lampas* at the reference site, pH_T 8.14 **(D)** and at the elevated pCO_2 site, pH_T 7.81 **(E)**. Note extensive coverage of encrusting organisms and intact apex region. At the elevated pCO_2 site shells had a smooth bare shell surface and severely eroded apex regions (arrow).

used as the input variables, alongside the disassociation constants from Mehrbach et al. (1973), as adjusted by Dickson and Millero (1987), KSO_4 using Dickson (1990), and total borate concentrations from Uppström (1974).

CT-Scanning, Analysis, and Data Extraction

All scans were performed with an Aquilion New PRIME/Focus Edition CT scanner (Toshiba Medical, Tokyo, Japan) at the Kochi Core Center Open Facility System (Kochi University, Japan). Specimens were scanned on a helical scanning mode with a tube voltage of 120 kV, a current of 100 mA, a field of view of 139.7 mm, an interval (slice) thickness of 0.5 mm, an exposure time of 0.5 s and a FC85 reconstruction philtre. The scans were stored in the DICOM format and analysed using the software OsiriX MD (Pixmeo SARL, Geneva, Switzerland). The data comprised of a series of 0.5 mm slices (ranging from a total of 241–471 slices, depending on the length of the specimen) that followed the central axis of the columella. Each slice represents a cross section of the shell, from which it is possible to extract mean density (Hounsfield unit, HU) and shell thickness (mm). Different densities were converted from greyscale to colour using the "Hue 2" colour look up table in OsiriX MD.

Since it was expected that ocean acidification would result in smaller shells compared to the reference areas (Garilli et al., 2015; Harvey et al., 2016), we defined a number of shell regions based on discrete anatomical loci that could be located in all individuals, enabling comparison across individuals and treatments. These were the cross-sections located at the sutures on both ventral and dorsal side, the mid-point of the shell lip, and at the mid-point of the siphonal canal (see **Figure 3C**). For each of these shell regions, the corresponding slice was identified (1 slice per region) and used for subsequent analysis. To get a representative measure of

TABLE 1 | Carbonate chemistry conditions of the reference pCO_2 site (REF), and elevated pCO_2 site (ACID) at Shikine-jima, Japan.

Site	pH_T	Temp (°C)	Salinity (psu)	A_T (μmol kg^{-1})	pCO_2 (μatm)	DIC (μmol kg^{-1})	HCO_3^- (μmol kg^{-1})	CO_3^{2-} (μmol kg^{-1})	CO_2 (μmol kg^{-1})	$\Omega_{calcite}$	$\Omega_{aragonite}$
REF	8.137	19.73	34.50	2265.4	309.21	1963.69	1741.53	212.07	10.09	5.09	3.30
	0.056	0.71	0.43	15.4	46.44	34.39	55.11	22.23	1.54	0.53	0.35
ACID	7.809	19.47	34.07	2269.5	768.55	2129.81	1991.81	112.75	25.25	2.71	1.76
	0.093	0.82	0.69	20.3	225.24	33.29	44.37	17.90	7.07	0.43	0.28

The pH_T, temperature, salinity, and total alkalinity (A_T) are measured values. All other values were calculated using the carbonate chemistry system analysis program CO2SYS: Seawater pCO_2, dissolved inorganic carbon (DIC), bicarbonate (HCO_3^-), carbonate (CO_3^{2-}), carbon dioxide (CO_2), saturation states for calcite ($\Omega_{calcite}$), and aragonite ($\Omega_{aragonite}$). Values are presented as mean, with standard deviation below.

the density and thickness of the shell at the respective regions, an average was obtained for each identified slice; this involved overlaying 16 equally spaced radii (22.5°) from the centre of each slice, and extracting the mean density (Hounsfield unit, HU) and thickness (mm) where the radii overlapped with the shell (see **Figure 3D** for an example). Where dissolution had resulted in shell absence, both density and thickness were recorded as zero for that radius.

Statistical analysis of the changes in thickness and density were assessed using a repeated measures ANOVA in *R* (R Development Core Team, 2017) with the *treatment* (two levels; reference or elevated pCO_2) and *shell region* (12 levels; 1a, 1b, 2a. . .5b, shell lip, siphonal canal, see **Figure 3C** for more details) used as *between-subjects* factor, and the *shell region* for a given *individual* used as a *within-subjects* factor (or error term). Each *shell region* was then compared pairwise between the two levels of *treatment* as a planned contrast using a Bonferroni-corrected *t*-test. Normality was assessed using Q-Q plots. A Greenhouse-Geisser correction (which corrects for Type I error by reducing the degrees of freedom) was applied to the *within-subjects* factor of the repeated measures ANOVA to correct for potential issues of sphericity.

Geometric Morphometric Surface Analysis

A 3D surface rendering of each individual was compiled using the OsiriX MD software, exported as a surface mesh file (*.PLY file), and then imported into the "Generalized Procrustes Surface Analysis" (GPSA) software (Pomidor et al., 2016). The free and open source GPSA software was downloaded from the lab website (URL: http://morphlab.sc.fsu.edu/index.html, accessed October 5, 2017). The GPSA software can calculate differences in the shape of the surface between specimens by using the 3D surface rendering to carry out a superimposition on a metric termed "Procrustes surface metric" (PSM). This metric and approach, while relatively new, are analogous to the traditional geometric morphometric approach which uses Procrustes distance. Since this approach utilises a surface mesh, it is not possible to take the density into consideration. The programme itself allocates, by default, 4 GB of maximum memory for programme use; however, due to the large size of the surface mesh files, it was necessary to increase this to 8 GB. In order to perform the GPSA, the user must define the "prototype file" (the single surface file on which to base the superimposition), and the "surface files" to be analysed (which can also include the individual used for the "prototype file").

In order to test for group differences in the average shape of the surface between the reference- and elevated-CO_2 individuals, all 20 individuals were used as the "surface files" and a reference-CO_2 individual (chosen for being closest to the average shell length for reference individuals) was used as the "prototype file." The GPSA software then produces a square, symmetric matrix of the (PSM) distance between all 20 of the specimens, which was then compared using non-metric multidimensional scaling (nMDS). Additionally, by comparing all of the specimens' relative to a "mean" individual it is possible to project a heatmap

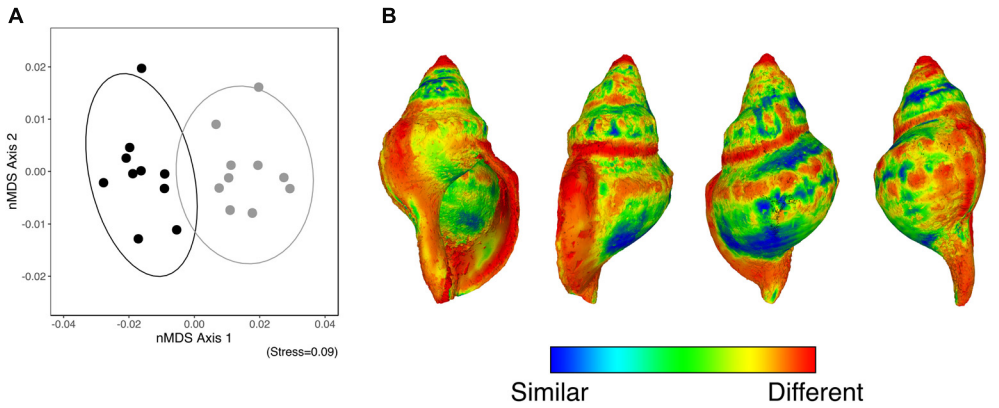

FIGURE 2 | (A) An nMDS ordination of the surface shape differences [based on the Generalized Procrustes Surface Analysis (GPSA)] between the control pCO_2 (solid black) and elevated pCO_2 (solid grey) individuals. **(B)** A heatmap of the differences in the shape of the surface based on the GPSA which highlights where the changes are most prominent between the elevated- and the mean shape of the reference pCO_2 individuals (where blue indicates a similar shape, and red indicates a greater degree of change).

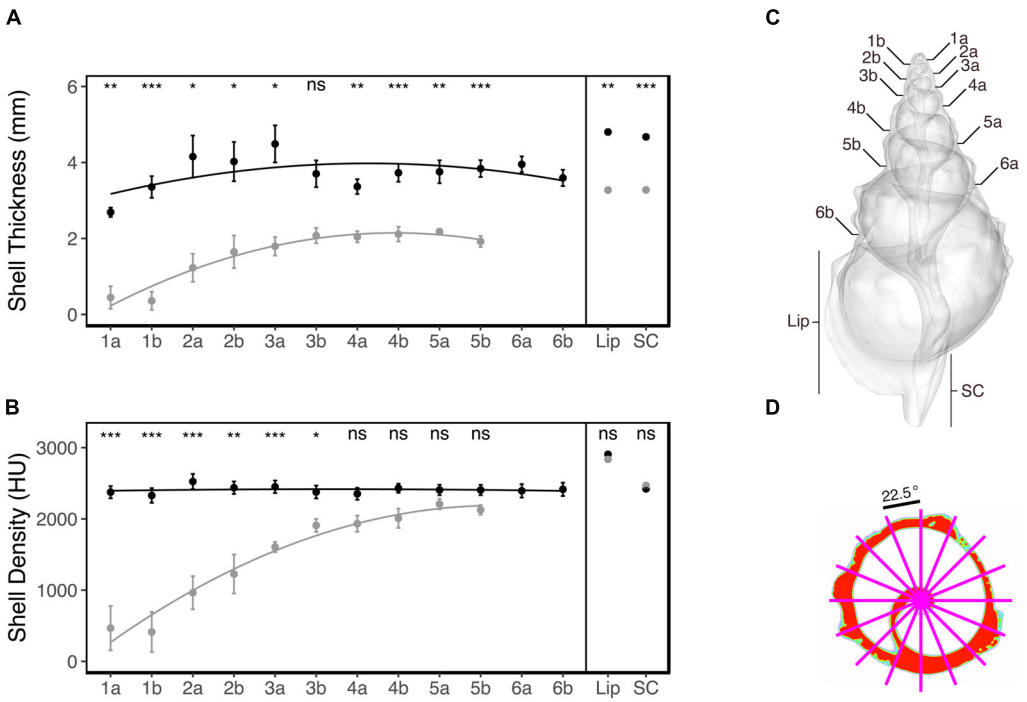

FIGURE 3 | Mean (±SE) shell thickness, mm **(A)** and mean (±SE) shell density, Hounsfield unit (HU) **(B)** of the control pCO_2 (solid black) and elevated pCO_2 (solid grey) individuals (n = 10) across the different shell regions. Pairwise comparisons for the same shell region were tested using a Bonferroni-corrected t-test, with the test results indicated at the top as (ns, non-significant, $*p < 0.05$, $**p < 0.01$, or $***p < 0.001$). The different shell regions (the dorsal "a" and ventral "b" sides of sutures 1–6, and the mid-points of the shell lip "lip" and siphonal canal "SC") are defined for a representative individual **(C)**. Average density and thickness was obtained for each shell region by overlaying 16 equally spaced radii (22.5°) from the centre of each slice, and extracting the mean density (HU) and thickness (mm) where the radii and shell intersected **(D)**.

on the "mean" shell which displays the average shape of the surface with the locations coloured to reflect the most prominent change (Pomidor et al., 2016). In order to ascertain how the elevated-CO_2 individuals differed from the reference-CO_2 individuals, we first created the "mean" reference shape. This involved using the GPSA software with just the 10 reference-CO_2 individuals (using the same "prototype" reference individual as above). The heatmap of the elevated-CO_2 individuals against the "mean" reference individual was then performed by re-running the GPSA with the elevated-CO_2 individual as the "surface files" and the newly created "mean" reference individual as the prototype.

RESULTS

Shells of *C. lampas* were visually distinguishable between the reference and high-CO_2 sites (**Figures 1D,E**). Individuals collected in the elevated pCO_2 area were smaller (mean shell length 177.6 ± 19.2 [SD] mm (n = 10) in reference pCO_2 and 112.0 ± 13.5 [SD] mm (n = 10) in elevated pCO_2; $F_{1,18}$ = 78.34, p < 0.001; see **Figures 1D,E**). The high-CO_2 individuals also had no epiphytes revealing a predominantly white shell colouration that was highly conspicuous against the substratum (**Figures 1D,E**), with damage and/or truncation to the apex and older shells regions (**Figure 1D**). On the contrary, individuals from the reference pCO_2 areas were much better camouflaged by a dark periostracum and an extensive cover of epiphytes (mainly crustose coralline algae) (**Figure 1E**). The surface of shells from the elevated pCO_2 area was smoother, with the shell lip, whorl shoulders, and stepping at suture lines more rounded in comparison to individuals from the reference area.

The GPSA demonstrated that along the axis of greatest variation (nMDS axis 1), the shape of the surface of those individuals collected from the elevated pCO_2 area contrasted with those collected from the reference pCO_2 (**Figure 2A**). **Figure 2B** shows the average shape of the surface of all individuals (from the four sides) alongside a heatmap which highlights where the changes are most prominent between the elevated-CO_2 individuals and the mean reference pCO_2 shell shape (where blue indicates a similar shape, and red indicates a greater degree of change). This shows that elevated levels of pCO_2 influenced mean shell shape, with the regions that differed the most being the apex, shell lip, and suture lines.

The CT-scanning analysis indicated that the shell thickness of individuals from the elevated pCO_2 areas were (on average) more than two times thinner compared to the reference pCO_2 areas (ANOVA *treatment:* $F_{1,204}$ = 27.18, p < 0.001; **Figure 3A**). This reduced thickness did not significantly interact with the shell region [ANOVA *treatment* × *shell region* (Greenhouse-Geisser corrected): $F_{3.04,47.74}$ = 0.66, p = 0.581; **Figure 3A**] meaning that the shell thickness was significantly thinner for almost all the shell regions of the elevated pCO_2 individuals (see **Figure 3A** for the pair-wise t-test results). This was regardless of whether the shell was newly grown (e.g., **Figure 4** – shell region 4b and shell lip) or older (e.g., **Figure 4** – shell regions 1a and 3a, see **Figure 3C** for shell region positions). See **Supplementary Table S1** for the full statistical analysis output, and **Supplementary Table S2** for the pairwise comparisons of the same shell region for both shell thickness and density.

Mean shell density was relatively similar across all of the shell regions for the reference pCO_2 individuals (**Figure 3B**). Overall, the effects of elevated pCO_2 significantly reduced shell density (ANOVA *treatment*: $F_{1,204}$ = 32.24, p < 0.001; **Figure 3B**). The elevated pCO_2 individuals showed a gradient where the older shell regions (1a to 3b; see **Figure 3C**) demonstrated a more than twofold reduction in mean density (**Figure 3B**), the intermediate shell regions (4a to 6b; see **Figure 3C**) showed a slightly reduced (but non-significant; t-test: p > 0.05) reduction, and the newly grown shell region (Lip and SC; see **Figure 3C**) showed an almost identical mean shell density compared to the reference pCO_2 individuals (**Figure 3B**). Representative examples of the CT cross-sections across the four shell regions (**Figure 4**) showed that the differences in shell density are more

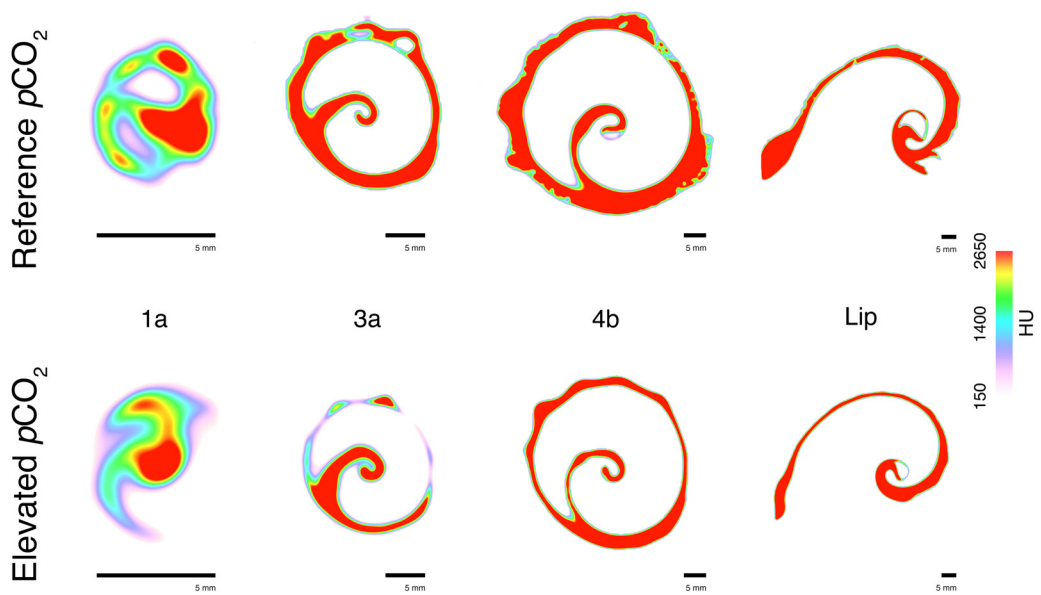

FIGURE 4 | Representative example of the identified cross-section slices from the computed tomography (CT) scanning from different shell regions (1a, 3a, 4b, and shell lip) collected from the reference pCO_2 **(Upper)** and elevated pCO_2 **(Lower)** sites. Colour scale indicates density (Hounsfield unit, HU) with warmer colours indicating higher density and cooler colours a lesser density.

prominent in the older shell regions (1a and 3a) compared to the newly grown shell regions (4b and Lip), with the most deteriorated areas demonstrating the lowest shell density (**Figures 3**, **4**).

DISCUSSION

Ocean acidification is one of the most pervasive environmental changes in the ocean (IPCC, 2013; Gattuso et al., 2015). Organisms with calcium carbonate shells or skeletons appear to be the most vulnerable to increasing levels of seawater pCO_2 (Harvey et al., 2013) and understanding their response is critical to assessments of the effects of rapidly falling carbonate saturation levels in coastal ecosystems. We have shown that chronic exposure to low seawater carbonate saturation caused corrosion to the shells of the widespread predatory Triton. Individuals in the high pCO_2 conditions were smaller than those in reference areas and they had clearly undergone progressive shell dissolution. The shells of *Charonia lampas* were smoother, thinner, and less dense. Damage caused by the low levels of aragonite saturation was greatest on the oldest shell parts; body tissues of some of these gastropods were exposed to the surrounding seawater through holes in the shell apex. Whilst calcification may not be the Achilles' heel of calcareous marine organisms, as many of them can upregulate their calcification rates in acidified conditions (Rodolfo-Metalpa et al., 2015), increased dissolution of both living and dead marine carbonates is one of the most profound risks of ocean acidification (McNeil and Matear, 2008); particularly since ocean acidification is causing the expansion of areas with periods of aragonite undersaturation (IPCC, 2013).

As ocean acidification continues worldwide, any ability of marine gastropods to achieve normal development will depend on their ability to maintain their growth and calcification, which demands tradeoffs in the allocation of available energy (Barry et al., 2011). The energetic costs of calcification may be increased under ocean acidification, for instance, due to the need to pump protons across cell membranes to control pH at sites of calcification (Ries, 2011; Toyofuku et al., 2017). This may require increased feeding to maintain their energy status (Sanford et al., 2014), or a repartitioning of energy between calcification, growth, reproduction, and maintenance (Wood et al., 2008; Stumpp et al., 2011; Waldbusser et al., 2013; Harvey and Moore, 2016; Harvey et al., 2016). It is likely that these responses may differ across the different life stages, with early stages often considered most sensitive to ocean acidification (see Byrne, 2011 for a review) as well as the potential for carry-over effects (e.g., Hettinger et al., 2013). Molluscs may be able to compensate for the negative effects of elevated pCO_2 if they can obtain enough food (Melzner et al., 2011; Thomsen et al., 2013), however, such compensatory effects may not always be possible (Harvey and Moore, 2016) with feeding behaviours potentially altered (Clements and Darrow, 2018). Evidence from CO_2 seeps suggests that food availability for predators may decrease as the size, recruitment and abundance of marine invertebrate prey is reduced in acidified conditions (Cigliano et al., 2010; Garilli et al., 2015; Harvey et al., 2016; Allen et al., 2017), resulting in limited trophic propagation to predator populations (Vizzini et al., 2017). This reduction in food availability might further compromise the available energy budget of marine organisms affected by ocean acidification. Should the available energy budget of organisms become compromised then it is possible that their reproductive contribution to future generations may also be reduced, with implications for species' abundances and distributions (Borregaard and Rahbek, 2010; Harvey et al., 2016).

Reductions in net calcification due to simulated ocean acidification have been observed in many gastropod species (Shirayama and Thornton, 2005; Gazeau et al., 2013; Parker et al., 2013; Queirós et al., 2015; Chatzinikolaou et al., 2016; Harvey and Moore, 2016; Harvey et al., 2016). For some species this reduced net calcification is due to erosion and dissolution of the shell rather than an inability to deposit new shell (e.g., Marshall et al., 2008; Nienhuis et al., 2010; Rodolfo-Metalpa et al., 2011). Live triton shells collected from the elevated pCO_2 area were on average almost half the size of those collected from the reference area, along with a consistently thinner shell, suggesting a physiological constraint on their ability to calcify. At the same time, *Charonia* spp. shells are comprised of aragonite and lack the less soluble outer calcitic layer found in some gastropods (Cubillas et al., 2005), implying an increased risk of dissolution under ocean acidification (Morse et al., 2007). We found that shell dissolution and deterioration in acidified conditions was most pronounced on the oldest parts of individuals. Similar observations of shell deterioration have been found for other gastropods under acidified conditions, including enhanced dissolution in the older shell parts, loss of the periostracum, and the general smoothing of the shell sculpture (e.g., whorl shoulders, axial and spiral riblets, and nodules) (Hall-Spencer et al., 2008; Marshall et al., 2008; Rodolfo-Metalpa et al., 2011; Queirós et al., 2015; Chatzinikolaou et al., 2016).

Changes in shell shape of the elevated pCO_2 individuals (as assessed by the geometric morphometric surface analysis) appeared to coincide with changes in thickness and density. These shape differences were predominantly found in the same areas of the shell that experienced large changes in thickness and/or density, such as the apex, sutures, and shell lip regions. Intuitively, the shell apex had an altered shape in the elevated-pCO_2 individuals with reduced shell density leading to the truncation (loss) of the apex for most individuals; the sutures' shape was likely changed due to the general smoothing and thinning of the shell resulting in a more simplified shape; and the thinning of the shell lip likely explained the changes in shape observed for that region. Overall, these changes suggest that ocean acidification will not simply reduce the rate of gross calcification for tritons, but instead suggests some extensive damage for a number of important regions of the shell. One mechanism through which molluscs can counteract physical and chemical damage to the shell is through shell repair, the secretion of carbonates onto the inner wall of the shell (Langer et al., 2014). When the shell wall is breached due to dissolution

(as observed here), the internal environment of the animal becomes compromised (Vermeij, 1983), with potential negative implications for calcification and shell repair. In the present study, there was no observable shell repair for the elevated-CO_2 individuals. The evidence for the effects of ocean acidification on the ability of molluscs to perform shell repair is mixed, ranging from successful thickening of the inner shell layers to counteract the negative effects (Langer et al., 2014; Peck et al., 2018), to negative effects on shell repair rate (Coleman et al., 2014).

Individuals in the elevated-CO_2 area showed a gradient in density that decreased from the newest to the oldest regions of the shell. While the oldest shell parts had a greatly reduced density, the density of the most recent shell growth, the growing lip of the shell aperture, and its siphonal canal, was similar in individuals from the reference and high pCO_2 areas. This implies that the gastropods are capable of producing the necessary shell material (albeit as a reduced rate), but that the quality of this material gets eroded and dissolved over time. We suggest that since the individuals here have been exposed for their entire lifetime, this is enough for this continuous dissolution to be discernible. Many ocean acidification studies include experiments with only a short duration of exposure (see Cornwall and Hurd, 2016 for a critique), these may have underestimated the impacts on gastropods by being of insufficient length to capture the potential extent of shell damage due to ocean acidification. Few studies have investigated changes in shell density due to ocean acidification, but those that have found that shell density in gastropods is negatively impacted (Queirós et al., 2015; Chatzinikolaou et al., 2016) resulting in weakened shells. Queirós et al. (2015) showed that ocean acidification caused apex truncation and reduction in the shell lip density for *Nucella lapillus*. Chatzinikolaou et al. (2016) found that the effects of reduced pH over a 3-month period caused a deterioration of the shell surface and a reduction in the shell density of gastropods *Nassarius nitidus* and *Columbella rustica*. We conclude that *C. lampas* are enduring a two-pronged impact whereby the acidified conditions are affecting these gastropods physiologically (e.g., through acid-base balance disturbances) hindering their ability to calcify (exhibited by their reduced size and thickness), with dissolution playing a key role in progressively impacting the quality (density) of the shell material over time.

There was a complete absence of epiphytic cover on triton shells living in seabed areas with elevated pCO_2, compared to a near-total epiphytic cover on those individuals from the reference area, which was predominantly covered in crustose coralline algae. Epiphytic cover of crustose coralline algae is highly susceptible to ocean acidification (Martin et al., 2008). It is possible for epibionts to negatively affect the basibiont upon which they are associated, for example; reducing light availability for autotrophs (Sand-Jensen, 1977), or increasing drag and reducing the growth rate of heterotrophs (Wahl, 1997). However, given that dissolution acts on external surfaces in direct contact with the seawater, the presence of epiphytes on the shell of an organism may provide a protective layer that alleviates dissolution rates. It is unclear as to the exact mechanism causing a lack of epiphytes, whether a direct sensitivity of the crustose coralline algae to the acidified conditions (Kuffner et al., 2007) or the dissolution of the shell surface precluding settlement. Regardless, the observed shell corrosion was almost certainly exacerbated by the absence of epiphytes. This emphasises the need to consider multi-species responses to ocean acidification.

The findings presented here highlight a number of broader ecological implications that ocean acidification will have for the predatory gastropod *C. lampas*. One consequence of the elevated pCO_2 was the lack of epiphytes and concurrent discolouration of the shell. Typically, the presence of epiphytes on *C. lampas* individuals provides a form of cryptic coloration hiding them from prey and predators alike, whereas the lack of epiphytes and white shell colouration make individuals highly conspicuous in the elevated pCO_2 area. The severe dissolution of older shell regions, and reduced density and thickness of the shell will also result in structural weakness, as shown for barnacle tests (McDonald et al., 2009) and serpulids tubes (Chan et al., 2012). These changes in colour and mechanical strength may make them more vulnerable to predators or may increase predator avoidance behaviours at the expense of other important biological and ecological processes (e.g., feeding and reproduction; see Clements and Hunt, 2015 for a review). An altered competitive dynamic with other species, and the possible reduction in their top-down control, would likely disrupt their associated food web, and may alter ecosystem processes and derived services (Lemasson et al., 2017). For example, the giant triton (*C. tritonis*) plays an important role in the tropics as one of the very few natural predators of the coral-eating crown-of-thorns starfish (*Acanthaster planci*), which is a major contributor to ongoing coral loss on reefs across the Indo-Pacific (Pratchett et al., 2017).

Carbon dioxide seeps provide useful analogues for investigating the effects of ocean acidification since they allow the consideration of both direct and indirect ecological effects in a natural setting across different life-stages (Hall-Spencer et al., 2008; Fabricius et al., 2011; Agostini et al., 2018). The current study investigated the long-term responses of a large predatory gastropod to ocean acidification using CT-scanning on individuals collected from a shallow-water Japanese CO_2 seep. Chronic exposure to ocean acidification, and periodic exposure to aragonite undersaturation hinders the ability of *C. lampas* to produce and maintain their $CaCO_3$ shells. While net calcification was reduced in response to ocean acidification, shell dissolution was the predominant impact and cause of corrosion and reduced shell density. Even though many marine organisms are able to upregulate calcification rates to counter ocean acidification, they may not be able to maintain their shells or skeletons due to dissolution. Those studies that only consider effects of rising CO_2 levels on calcification underestimate the impacts of ocean acidification. In summary, this study highlights the need to consider both carbonate dissolution and deposition rates in order to understand the effects of ocean acidification on marine organisms.

ETHICS STATEMENT

The study was exempt from ethical approval procedures as the study organism was an invertebrate animal, *Charonia lampas*, from Phylum Mollusca, Class Gastropoda.

AUTHOR CONTRIBUTIONS

BH conceived the idea and wrote the manuscript in collaboration with SA, SW, KI, and JH-S. BH, SA, SW, and JH-S conducted the specimen collection at the study site. BH performed the computed tomography scanning analyses. All authors read and commented on the manuscript.

FUNDING

This project was supported by the Sasakawa Scientific Research Grant from The Japan Science Society (Project No. 29-745) awarded to BH and contributes toward the "International Education and Research Laboratory Program", University of Tsukuba.

ACKNOWLEDGMENTS

We thank Yasutaka Tsuchiya and the technical staff at the "Shimoda Marine Research Center, University of Tsukuba" for their assistance at the study site. We also thank Kazuno Arai from the "Kochi Core Center Open Facility System" at Kochi University for providing access to the Aquilion New PRIME/Focus Edition CT scanner and her assistance in the CT-scanning. Finally, we recognise Dr. Shunsuke Yaguchi of "Shimoda Marine Research Center, University of Tsukuba" for his assistance and support in the associated funding applications.

SUPPLEMENTARY MATERIAL

The Supplementary Material for this article can be found online at: https://www.frontiersin.org/articles/10.3389/fmars.2018.00371/full#supplementary-material

REFERENCES

Agostini, S., Harvey, B. P., Wada, S., Kon, K., Milazzo, M., Inaba, K., et al. (2018). Ocean acidification drives community shifts towards simplified non-calcified habitats in a subtropical-temperate transition zone. *Sci. Rep.* 8:11354. doi: 10.1038/s41598-018-29251-7

Allen, R., Foggo, A., Fabricius, K., Balistreri, A., and Hall-Spencer, J. M. (2017). Tropical CO2 seeps reveal the impact of ocean acidification on coral reef invertebrate recruitment. *Mar. Pollut. Bull.* 124, 607–613. doi: 10.1016/j.marpolbul.2016.12.031

Bach, L. T. (2015). Reconsidering the role of carbonate ion concentration in calcification by marine organisms. *Biogeosciences* 12, 4939–4951. doi: 10.5194/bg-12-4939-2015

Barry, J. P., Widdicombe, S., and Hall-Spencer, J. M. (2011). "Effects of ocean acidification on marine biodiversity and ecosystem function," in *Ocean Acidification*, eds J. P. Gattuso, and L. Lansson (Oxford: Oxford University Press), 192–209.

Borregaard, M. K., and Rahbek, C. (2010). Causality of the relationship between geographic distribution and species abundance. *Q. Rev. Biol.* 85, 3–25.

Byrne, M. (2011). Impact of ocean warming and ocean acidification on marine invertebrate life history stages: vulnerabilities and potential for persistence in a changing ocean. *Ocean. Mar. Biol.* 49, 1–42.

Caldeira, K., and Wickett, M. E. (2003). Oceanography: anthropogenic carbon and ocean pH. *Nature* 425:365. doi: 10.1038/425365a

Chan, V. B. S., Li, C., Lane, A. C., Wang, Y., Lu, X., Shih, K., et al. (2012). CO2-driven ocean acidification alters and weakens integrity of the calcareous tubes produced by the Serpulid tubeworm, *Hydroides elegans*. *PLOS One* 7:e42718. doi: 10.1371/journal.pone.0042718

Chatzinikolaou, E., Grigoriou, P., Keklikoglou, K., Faulwetter, S., Papageorgiou, N., and Norkko, J. (2016). The combined effects of reduced pH and elevated temperature on the shell density of two gastropod species measured using micro-CT imaging. *ICES J. Mar. Sci.* 74, 1135–1149. doi: 10.1093/icesjms/fsw219

Cigliano, M., Gambi, M. C., Rodolfo-Metalpa, R., Patti, F. P., and Hall-Spencer, J. M. (2010). Effects of ocean acidification on invertebrate settlement at volcanic CO2 vents. *Mar. Biol.* 157, 2489–2502. doi: 10.1007/s00227-010-1513-6

Clements, J. C., and Darrow, E. S. (2018). Eating in an acidifying ocean: a quantitative review of elevated CO2 effects on the feeding rates of calcifying marine invertebrates. *Hydrobiologia* 820, 1–21. doi: 10.1007/s10750-018-3665-1

Clements, J. C., and Hunt, H. L. (2015). Marine animal behaviour in a high CO2 ocean. *Mar. Ecol. Prog. Ser.* 536, 259–279.

Cohen, A. L., and Holcomb, M. (2009). Why corals care about ocean acidification: uncovering the mechanism. *Oceanography* 22, 118–127. doi: 10.5670/oceanog.2009.102

Coleman, D. W., Byrne, M., and Davis, A. R. (2014). Molluscs on acid: gastropod shell repair and strength in acidifying oceans. *Mar. Ecol. Prog. Ser.* 509, 203–211.

Cornwall, C. E., and Hurd, C. L. (2016). Experimental design in ocean acidification research: problems and solutions. *ICES J. Mar. Sci.* 73, 572–581. doi: 10.1093/icesjms/fsv118

Cubillas, P., Köhler, S., Prieto, M., Chaïrat, C., and Oelkers, E. H. (2005). Experimental determination of the dissolution rates of calcite, aragonite, and bivalves. *Chem. Geol.* 216, 59–77. doi: 10.1016/j.chemgeo.2004.11.009

Cyronak, T., Schulz, K. G., and Jokiel, P. L. (2016). Response to Waldbusser et al. (2016): "Calcium carbonate saturation state: on myths and this or that stories." *ICES J. Mar. Sci.* 73, 569–571. doi: 10.1093/icesjms/fsv224

Dickson, A. G. (1990). Thermodynamics of the dissociation of boric acid in potassium chloride solutions from 273.15 to 318.15 K. *J. Chem. Eng. Data* 35, 253–257. doi: 10.1021/je00061a009

Dickson, A. G., and Millero, F. J. (1987). A comparison of the equilibrium constants for the dissociation of carbonic acid in seawater media. *Deep Sea Res. Part Oceanogr. Res. Pap.* 34, 1733–1743. doi: 10.1016/0198-0149(87)90021-5

Fabricius, K. E., Langdon, C., Uthicke, S., Humphrey, C., Noonan, S., De'ath, G., et al. (2011). Losers and winners in coral reefs acclimatized to elevated carbon dioxide concentrations. *Nat. Clim. Change* 1, 165–169. doi: 10.1038/nclimate1122

Feely, R. A., Sabine, C. L., Hernandez-Ayon, J. M., Ianson, D., and Hales, B. (2008). Evidence for upwelling of corrosive "acidified" water onto the continental shelf. *Science* 320, 1490–1492. doi: 10.1126/science.1155676

Fitzer, S. C., Phoenix, V. R., Cusack, M., and Kamenos, N. A. (2014). Ocean acidification impacts mussel control on biomineralisation. *Sci. Rep.* 4:6218. doi: 10.1038/srep06218

Garilli, V., Rodolfo-Metalpa, R., Scuderi, D., Brusca, L., Parrinello, D., Rastrick, S. P. S., et al. (2015). Physiological advantages of dwarfing in surviving extinctions in high-CO2 oceans. *Nat. Clim. Change* 5, 678–682. doi: 10.1038/nclimate2616

Gattuso, J.-P., Magnan, A., Billé, R., Cheung, W. W. L., Howes, E. L., Joos, F., et al. (2015). Contrasting futures for ocean and society from different anthropogenic CO2 emissions scenarios. *Science* 349:aac4722. doi: 10.1126/science.aac4722

Gazeau, F., Parker, L. M., Comeau, S., Gattuso, J.-P., O'Connor, W. A., Martin, S., et al. (2013). Impacts of ocean acidification on marine shelled molluscs. *Mar. Biol.* 160, 2207–2245. doi: 10.1007/s00227-013-2219-3

Hall-Spencer, J. M., Rodolfo-Metalpa, R., Martin, S., Ransome, E., Fine, M., Turner, S. M., et al. (2008). Volcanic carbon dioxide vents show ecosystem effects of ocean acidification. *Nature* 454, 96–99. doi: 10.1038/nature07051

Harvey, B. P., Al-Janabi, B., Broszeit, S., Cioffi, R., Kumar, A., Aranguren-Gassis, M., et al. (2014). Evolution of marine organisms under climate change at different levels of biological organisation. *Water* 6, 3545–3574. doi: 10.3390/w6113545

Harvey, B. P., Gwynn-Jones, D., and Moore, P. J. (2013). Meta-analysis reveals complex marine biological responses to the interactive effects of ocean acidification and warming. *Ecol. Evol.* 3, 1016–1030. doi: 10.1002/ece3.516

Harvey, B. P., McKeown, N. J., Rastrick, S. P. S., Bertolini, C., Foggo, A., Graham, H., et al. (2016). Individual and population-level responses to ocean acidification. *Sci. Rep.* 6:20194. doi: 10.1038/srep20194

Harvey, B. P., and Moore, P. J. (2016). Ocean warming and acidification prevents compensatory response in a predator to reduced prey quality. *Mar. Ecol. Prog. Ser.* 563, 111–122. doi: 10.3354/meps11956

Hettinger, A., Sanford, E., Hill, T. M., Lenz, E. A., Russell, A. D., and Gaylord, B. (2013). Larval carry-over effects from ocean acidification persist in the natural environment. *Glob. Change Biol.* 19, 3317–3326. doi: 10.1111/gcb.12307

Inoue, S., Kayanne, H., Yamamoto, S., and Kurihara, H. (2013). Spatial community shift from hard to soft corals in acidified water. *Nat. Clim. Change* 3, 683–687. doi: 10.1038/nclimate1855

IPCC (2013). *Climate Change 2013 - The Physical Science Basis: Working Group I Contribution to the Fifth Assessment Report of the IPCC*. Cambridge: Cambridge University Press.

Kang, K. H., and Kim, J. M. (2004). The predation of trumpet shell, *Charonia* sp., on eight different marine invertebrate species. *Aquac. Res.* 35, 1202–1206. doi: 10.1111/j.1365-2109.2004.01124.x

Kohn, A. J., Myers, E. R., and Meenakshi, V. (1979). Interior remodeling of the shell by a gastropod mollusc. *Proc. Natl. Acad. Sci. U.S.A.* 76, 3406–3410.

Kroeker, K. J., Kordas, R. L., Crim, R., Hendriks, I. E., Ramajo, L., Singh, G. S., et al. (2013). Impacts of ocean acidification on marine organisms: quantifying sensitivities and interaction with warming. *Glob. Change Biol.* 19, 1884–1896. doi: 10.1111/gcb.12179

Kuffner, I. B., Andersson, A. J., Jokiel, P. L., Rodgers, K. S., and Mackenzie, F. T. (2007). Decreased abundance of crustose coralline algae due to ocean acidification. *Nat. Geosci.* 1, 114–117. doi: 10.1038/ngeo100

Langer, G., Nehrke, G., Baggini, C., Rodolfo-Metalpa, R., Hall-Spencer, J. M., and Bijma, J. (2014). Limpets counteract ocean acidification induced shell corrosion by thickening of aragonitic shell layers. *Biogeosciences* 11, 7363–7368. doi: 10.5194/bg-11-7363-2014

Lemasson, A. J., Fletcher, S., Hall-Spencer, J. M., and Knights, A. M. (2017). Linking the biological impacts of ocean acidification on oysters to changes in ecosystem services: a review. *J. Exp. Mar. Biol. Ecol.* 492, 49–62. doi: 10.1016/j.jembe.2017.01.019

Marshall, D. J., Santos, J. H., Leung, K. M. Y., and Chak, W. H. (2008). Correlations between gastropod shell dissolution and water chemical properties in a tropical estuary. *Mar. Environ. Res.* 66, 422–429. doi: 10.1016/j.marenvres.2008.07.003

Martin, S., Rodolfo-Metalpa, R., Ransome, E., Rowley, S., Buia, M.-C., Gattuso, J.-P., et al. (2008). Effects of naturally acidified seawater on seagrass calcareous epibionts. *Biol. Lett.* 4, 689–692. doi: 10.1098/rsbl.2008.0412

McDonald, M. R., McClintock, J. B., Amsler, C. D., Rittschof, D., Angus, R. A., Orihuela, B., et al. (2009). Effects of ocean acidification over the life history of the barnacle *Amphibalanus amphitrite*. *Mar. Ecol. Prog. Ser.* 385, 179–187. doi: 10.3354/meps08099

McNeil, B. I., and Matear, R. J. (2008). Southern Ocean acidification: a tipping point at 450-ppm atmospheric CO2. *Proc. Natl. Acad. Sci. U.S.A.* 105, 18860–18864. doi: 10.1073/pnas.0806318105

Mehrbach, C., Culberson, C. H., Hawley, J. E., and Pytkowicz, R. M. (1973). Measurement of the apparent dissociation constants of carbonic acid in seawater at atmospheric pressure. *Limnol. Oceanogr.* 18, 897–907. doi: 10.4319/lo.1973.18.6.0897

Melzner, F., Stange, P., Trübenbach, K., Thomsen, J., Casties, I., Panknin, U., et al. (2011). Food supply and seawater pCO2 impact calcification and internal shell dissolution in the blue mussel Mytilus edulis. *PLOS One* 6:e24223. doi: 10.1371/journal.pone.0024223

Morse, J. W., and Arvidson, R. S. (2002). The dissolution kinetics of major sedimentary carbonate minerals. *Earth Sci. Rev.* 58, 51–84. doi: 10.1016/S0012-8252(01)00083-6

Morse, J. W., Arvidson, R. S., and Lüttge, A. (2007). Calcium carbonate formation and dissolution. *Chem. Rev.* 107, 342–381. doi: 10.1021/cr050358j

Nagelkerken, I., and Connell, S. D. (2015). Global alteration of ocean ecosystem functioning due to increasing human CO2 emissions. *Proc. Natl. Acad. Sci. U.S.A.* 112, 13272–13277. doi: 10.1073/pnas.1510856112

Nienhuis, S., Palmer, A. R., and Harley, C. D. G. (2010). Elevated CO2 affects shell dissolution rate but not calcification rate in a marine snail. *Proc. R. Soc. B Biol. Sci.* 277, 2553–2558. doi: 10.1098/rspb.2010.0206

Parker, L. M., Ross, P. M., O'Connor, W. A., Pörtner, H. O., Scanes, E., and Wright, J. M. (2013). Predicting the response of molluscs to the impact of ocean acidification. *Biology* 2, 651–692. doi: 10.3390/biology2020651

Peck, V. L., Oakes, R. L., Harper, E. M., Manno, C., and Tarling, G. A. (2018). Pteropods counter mechanical damage and dissolution through extensive shell repair. *Nat. Commun.* 9:264. doi: 10.1038/s41467-017-02692-w

Pierrot, D., Lewis, E., and Wallace, D. W. R. (2006). *MS Excel Program Developed for CO2 System Calculations, ORNL/CDIAC-105*. Oak Ridge, Tenn: Oak Ridge National Laboratory.

Pomidor, B. J., Makedonska, J., and Slice, D. E. (2016). A landmark-free method for three-dimensional shape analysis. *PLOS One* 11:e0150368. doi: 10.1371/journal.pone.0150368

Pratchett, S. M., Caballes, F. C., Wilmes, C. J., Matthews, S., Mellin, C., Sweatman, P. H., et al. (2017). Thirty years of research on Crown-of-Thorns Starfish (1986–2016): Scientific advances and emerging opportunities. *Diversity* 9:41. doi: 10.3390/d9040041

Queirós, A. M., Fernandes, J. A., Faulwetter, S., Nunes, J., Rastrick, S. P. S., Mieszkowska, N., et al. (2015). Scaling up experimental ocean acidification and warming research: from individuals to the ecosystem. *Glob. Change Biol.* 21, 130–143. doi: 10.1111/gcb.12675

R Development Core Team (2017). *R: A Language and Environment for Statistical Computing*. Vienna: R Foundation for Statistical Computing.

Raven, J., Caldeira, K., Elderfield, H., Hoegh-Guldberg, O., Liss, P., Riebesell, U., et al. (2005). *Ocean Acidification Due to Increasing Atmospheric Carbon Dioxide*. London: The Royal Society.

Ries, J. B. (2011). A physicochemical framework for interpreting the biological calcification response to CO2-induced ocean acidification. *Geochim. Cosmochim. Acta* 75, 4053–4064. doi: 10.1016/j.gca.2011.04.025

Ries, J. B., Cohen, A. L., and McCorkle, D. C. (2009). Marine calcifiers exhibit mixed responses to CO2-induced ocean acidification. *Geology* 37, 1131–1134. doi: 10.1130/G30210A.1

Rodolfo-Metalpa, R., Houlbrèque, F., Tambutté, É, Boisson, F., Baggini, C., Patti, F. P., et al. (2011). Coral and mollusc resistance to ocean acidification adversely affected by warming. *Nat. Clim. Change* 1, 308–312. doi: 10.1038/nclimate1200

Rodolfo-Metalpa, R., Montagna, P., Aliani, S., Borghini, M., Canese, S., Hall-Spencer, J. M., et al. (2015). Calcification is not the Achilles' heel of cold-water corals in an acidifying ocean. *Glob. Change Biol.* 21, 2238–2248. doi: 10.1111/gcb.12867

Roleda, M. Y., Boyd, P. W., and Hurd, C. L. (2012). Before ocean acidification: calcifier chemistry lessons. *J. Phycol.* 48, 840–843. doi: 10.1111/j.1529-8817.2012.01195.x

Sand-Jensen, K. (1977). Effect of epiphytes on eelgrass photosynthesis. *Aquat. Bot.* 3, 55–63. doi: 10.1016/0304-3770(77)90004-3

Sanford, E., Gaylord, B., Hettinger, A., Lenz, E. A., Meyer, K., and Hill, T. M. (2014). Ocean acidification increases the vulnerability of native oysters to predation by invasive snails. *Proc. R. Soc. B Biol. Sci.* 281:20132681. doi: 10.1098/rspb.2013.2681

Shirayama, Y., and Thornton, H. (2005). Effect of increased atmospheric CO2 on shallow water marine benthos. *J. Geophys. Res. Oceans* 110:C09S08. doi: 10.1029/2004JC002618

Stumpp, M., Hu, M. Y., Melzner, F., Gutowska, M. A., Dorey, N., Himmerkus, N., et al. (2012). Acidified seawater impacts sea urchin larvae pH regulatory systems

relevant for calcification. *Proc. Natl. Acad. Sci. U.S.A.* 109, 18192–18197. doi: 10.1073/pnas.1209174109

Stumpp, M., Wren, J., Melzner, F., Thorndyke, M. C., and Dupont, S. T. (2011). CO2 induced seawater acidification impacts sea urchin larval development I: elevated metabolic rates decrease scope for growth and induce developmental delay. *Comp. Biochem. Physiol. A Mol. Integr. Physiol.* 160, 331–340. doi: 10.1016/j.cbpa.2011.06.022

Sunday, J. M., Fabricius, K. E., Kroeker, K. J., Anderson, K. M., Brown, N. E., Barry, J. P., et al. (2017). Ocean acidification can mediate biodiversity shifts by changing biogenic habitat. *Nat. Clim. Change* 7, 81–85. doi: 10.1038/nclimate3161

Thomsen, J., Casties, I., Pansch, C., Körtzinger, A., and Melzner, F. (2013). Food availability outweighs ocean acidification effects in juvenile *Mytilus edulis*: laboratory and field experiments. *Glob. Change Biol.* 19, 1017–1027. doi: 10.1111/gcb.12109

Toyofuku, T., Matsuo, M. Y., de Nooijer, L. J., Nagai, Y., Kawada, S., Fujita, K., et al. (2017). Proton pumping accompanies calcification in foraminifera. *Nat. Commun.* 8:14145. doi: 10.1038/ncomms14145

Uppström, L. R. (1974). The boron/chlorinity ratio of deep-sea water from the Pacific Ocean. *Deep Sea Res. Oceanogr. Abstr.* 21, 161–162. doi: 10.1016/0011-7471(74)90074-6

Vermeij, G. J. (1983). Traces and trends of predation, with special reference to bivalved animals. *Palaeontology* 26, 455–465.

Vizzini, S., Martínez-Crego, B., Andolina, C., Massa-Gallucci, A., Connell, S. D., and Gambi, M. C. (2017). Ocean acidification as a driver of community simplification via the collapse of higher-order and rise of lower-order consumers. *Sci. Rep.* 7:4018. doi: 10.1038/s41598-017-03802-w

Wahl, M. (1997). Increased drag reduces growth of snails: comparison of flume and *in situ* experiments. *Mar. Ecol. Prog. Ser.* 151, 291–293. doi: 10.3354/meps151291

Waldbusser, G. G., Brunner, E. L., Haley, B. A., Hales, B., Langdon, C. J., and Prahl, F. G. (2013). A developmental and energetic basis linking larval oyster shell formation to acidification sensitivity. *Geophys. Res. Lett.* 40, 2171–2176. doi: 10.1002/grl.50449

Waldbusser, G. G., Hales, B., and Haley, B. A. (2016). Calcium carbonate saturation state: on myths and this or that stories. *ICES J. Mar. Sci.* 73, 563–568. doi: 10.1093/icesjms/fsv174

Wood, H. L., Spicer, J. I., and Widdicombe, S. (2008). Ocean acidification may increase calcification rates, but at a cost. *Proc. R. Soc. B Biol. Sci.* 275, 1767–1773. doi: 10.1098/rspb.2008.0343

Conflict of Interest Statement: The authors declare that the research was conducted in the absence of any commercial or financial relationships that could be construed as a potential conflict of interest.